

## Supporting Information

### **Fabrication of highly uniform gel-coatings by conversion of surface-anchored metal-organic frameworks**

M. Tsotsalas,<sup>1</sup> J. Liu,<sup>1</sup> B. Tettmann,<sup>1</sup> S. Grosjean,<sup>2,3</sup> A. Shahnas,<sup>1</sup> Z. Wang,<sup>1</sup> C. Azucena,<sup>1</sup> M. Addicoat,<sup>4</sup> T. Heine,<sup>4</sup> J. Lahann,<sup>1</sup> J. Overhage,<sup>1</sup> S. Bräse,<sup>2,5</sup> H. Gliemann,<sup>1</sup> C. Wöll<sup>1</sup>

<sup>1</sup> Institute of Functional Interfaces (IFG), Karlsruhe Institute of Technology (KIT), Hermann-von-Helmholtz-Platz 1, 76344 Eggenstein-Leopoldshafen, Germany

<sup>2</sup> Institute for Organic Chemistry (IOC), Karlsruhe Institute of Technology (KIT), Fritz-Haber-Weg 6, 76131 Karlsruhe, Germany

<sup>3</sup> Soft Matter Synthesis Lab, Institute for Biological Interfaces (IBG), Karlsruhe Institute of Technology (KIT), Hermann-von-Helmholtz-Platz 1, 76344 Eggenstein-Leopoldshafen, Germany

<sup>4</sup> Jacobs University Bremen, Center for Functional Nanomaterials, 28759 Bremen, Germany

<sup>5</sup> Institute of Toxicology and Genetics (ITG), Karlsruhe Institute of Technology (KIT), Hermann-von-Helmholtz-Platz 1, 76344 Eggenstein-Leopoldshafen, Germany

## Materials and Methods

S1 IRRAS spectra of the cross-linker, the free DA-SBDC linker and the cross-linked Cu-DA-SBDC SURMOF after EDTA treatment.

S2 IRRAS spectra of Cu-DA-SBDC SURMOF before and after EDTA treatment.

S3 EDX data of a cross-linked Cu-DA-SBDC SURMOF before and after EDTA treatment.

S4 In situ QCM analysis of the Cu ion removal via EDTA solution of a cross-linked Cu-DA-SBDC SURGEL.

S5 IRRAS spectrum of the QCM substrate after EDTA treatment.

S6 Simulated and experimental XRD data of a pillared-layer Cu-DA-SBDC-dabco SURMOF before and after cross-linking.

S7 IRRAS spectra of a pillared-layer Cu-DA-SBDC-dabco SURMOF before and after EDTA.

S8 Simulated structures of cross-linked SURMOFs Cu-DA-SBDC and Cu-DA-SBDC-dabco.

S9 Simulated and experimental XRD data of Cu-DA-SBDC SURMOF-2 before and after cross-linking.

S10 Fluorescent microscopy images of 5-cyano-2,3-ditolyt tetrazolium chloride (CTC) stained *P. putida* pJN::GFP after 24 h incubation in presence of arabinose loaded SURGELs and empty SURGEL.

S11 Fluorescent microscopy images of *E. coli* pJN::GFP after 24 h incubation in presence of arabinose loaded SURGELs and empty SURGEL and of 5-cyano-2,3-ditolyt tetrazolium chloride (CTC) stained bacteria settled on the empty SURGEL substrate.

S12 Microscopy images from the broth supernatant of both bacteria organisms after 24 h incubation in presence of arabinose loaded SURGELs.

S13 AFM image of a delaminated SURGEL sample after treatment in basic conditions.

## Materials and methods

All chemicals were purchased from commercial sources and used without any further purification if not indicated differently. 2,2'-diamino-4,4'-stilbenedicarboxylic acid was purchased from Sigma-Aldrich; tetrahydrofuran and trimethylsilylazide were purchased from Acros Organics; tert-butyl nitrite was purchased from ABCR; Trimethylolethane, propionic acid, *p*-Toluenesulfonic acid monohydrate and toluene were purchased from Alfa Aesar and were used as received.

**X-ray Diffraction (XRD).** XRD was carried out on a Bruker D8 Advance in  $\theta$ - $2\theta$  geometry equipped with a Si-strip detector (PSD Lynxeye (C)) using Cu K $_{\alpha}$ 1,2 radiation. On the tube side, a variable divergence slit set to V12 (fixed slit with 12 mm opening) and on the receiving side a 2.5° Soller slit was used. Scans ran from 4° to 20° ( $2\theta$ ) with a step width of 0.024° and 2 seconds per step, which resulted in a total step counting time of 178 seconds due to the specific PSD settings. Evaluation of data was done with Bruker evaluation software EVA 15.0. After background correction, the peak positions were calibrated using the position of the substrate Au(111) diffraction peak position, which was measured additionally at the end of each run.

**Infrared (IR) Spectroscopy.** The IRRA spectra were recorded on a Bruker VERTEX 80 FTIR spectrometer. Perdeuterated hexadecanethiol-SAMs on Au/Si were used for reference measurements. For DA-SBDC, IR spectrum was recorded with a FTIR Bruker IFS 88 spectrometer, using the attenuated total reflection technique (ATR). The absorption band positions are given in wave numbers  $\nu$  in  $\text{cm}^{-1}$ .

**Nuclear Magnetic Resonance (NMR) Spectroscopy.**  $^1\text{H}$  NMR (500 MHz) and  $^{13}\text{C}$  NMR (125 MHz) spectra were recorded on Bruker Avance III 500 spectrometer at room temperature with deuterated dimethyl sulfoxide ( $\text{DMSO}-d_6$ ). Chemical shifts,  $\delta$ , were quoted in parts per million (ppm) and were referenced to DMSO as internal standard. The following abbreviations were used to describe peak patterns when appropriate: br = broad, s = singlet, and d = doublet. Coupling constants,  $J$ , are reported in Hertz unit (Hz).

**High Resolution Mass Spectrometry (MS and HRMS).** Mass spectra were recorded with a Finnigan MAT 95 (70 eV) spectrometer under electron impact (EI) conditions. The molecular fragments were quoted as the relation between mass and charge ( $m/z$ ). The abbreviation  $[\text{M}^+]$  refers to the molecular ion.

**Synthesis of 2,2'-diazido-4,4'-stilbenedicarboxylic acid (DA-SBDC).** The synthetic procedure was adapted from literature.<sup>1</sup> 2,2'-diamino-4,4'-stilbenedicarboxylic acid (0.166 g, 0.56 mmol, 1 eq) was suspended in dry tetrahydrofuran (20 mL) in a dry 50 mL round-bottom flask. The suspension was cooled down to 0°C and tert-butyl nitrite (0.400 mL, 3.34 mmol, 6 eq) was added dropwise. After 15 minutes stirring trimethylsilylazide (0.293 mL, 2.23 mmol, 4 eq) was added dropwise at 0°C, and the reaction mixture was allowed to room temperature and stirred for 72 h. Tetrahydrofuran was evaporated under reduced pressure and the crude product was treated with a cold mixture of methanol and tetrahydrofuran (1/1, 20 mL), filtrated and dried *in vacuo* to give DA-SBDC (0.115 g, 0.33 mmol, 59%) as a yellow solid.

$^1\text{H-NMR}$  (500 MHz,  $\text{DMSO-}d_6$ ):  $\delta$  = 13.18 (br-s, 2H,  $\text{CO}_2\text{H}$ ), 7.90 (d, 2H,  $J$  = 8.0 Hz,  $\text{C}^{5/5'}\text{H}_{\text{Ar}}$ ), 7.76 (s, 2H,  $\text{HC=CH}$ ), 7.75 (d, 2H,  $J$  = 8.0 Hz,  $\text{C}^{6/6'}\text{H}_{\text{Ar}}$ ), 7.50 (s, 2H,  $\text{C}^{3/3'}\text{H}_{\text{Ar}}$ ) ppm.  $^{13}\text{C-NMR}$  (125 MHz,  $\text{DMSO-}d_6$ ):  $\delta$  = 166.2 ( $\text{CO}_2\text{H}$ ), 137.5 ( $\text{C}^{\text{IV}}$ ), 131.7 ( $\text{C}^{\text{IV}}$ ), 131.5 ( $\text{C}^{\text{IV}}$ ), 127.1 ( $\text{C}^{5/5'}\text{H}_{\text{Ar}}$ ), 125.9 ( $\text{C}^{6/6'}\text{H}_{\text{Ar}}$ ), 125.7 ( $\text{C}^{3/3'}\text{H}_{\text{Ar}}$ ), 119.7 ( $\text{HC=CH}$ ) ppm. IR (ATR):  $\nu$  = 3042, 2125, 1689, 1612, 1575, 1447, 1390, 1272, 1241  $\text{cm}^{-1}$ . MS (EI)  $m/z$  = 350 [ $\text{M}^+$ ], 322 [ $\text{M}^+-\text{N}_2$ ], 294 [ $\text{M}^+-\text{N}_4$ ], 249 [ $\text{M}^+-\text{CO}_2\text{H-N}_2$ ]. HRMS (EI)  $m/z$   $\text{C}_{16}\text{H}_{10}\text{N}_6\text{O}_4$ , calcd.: 350.0764, found: 350.0760.

**Synthesis of trimethylolethane tripropiolate:** The synthetic procedure was adapted from literature.<sup>2</sup> In a dry 250 mL round-bottom flask equipped with a Dean-Stark trap and magnetic stirring bar was placed trimethylolethane (1.0 g, 8.30 mmol) and *p*-Toluenesulfonic acid monohydrate (0.1 eq, 160 mg, 0.83 mmol) dissolved in dry 70 mL toluene. Propiolic acid (3.3 eq, 1.9 g, 27.4 mmol) was added dropwise, and then the mixture was heated to reflux. After 2 h the light brown solution was cooled to room temperature, 70 mL of ethyl acetate was added and washed twice with 5% sodium hydroxide solution (2 x 20 mL) then with brine solution (20 mL). Thereafter the product was dried over anhydrous magnesium sulfate, filtered and concentrated *in vacuo* yielding 2.1 g (7.61 mmol, 91%) of tripropiolate as a slightly yellow oil.

$^1\text{H-NMR}$  (500 MHz,  $\text{DMSO-}d_6$ ):  $\delta$  = 4.63 (s, 3H,  $\text{C}\equiv\text{CH}$ ), 4.13 (s, 6H,  $\text{CH}_2\text{O}$ ), 0.98 (s, 3H,  $\text{CH}_3$ ), ppm.  $^{13}\text{C-NMR}$  (125 MHz,  $\text{DMSO-}d_6$ ):  $\delta$  = 152.5 ( $\text{C=O}$ ), 80.1 ( $\text{C}\equiv\text{C}$ ), 74.8 ( $\text{C}\equiv\text{C}$ ), 23.1 ( $\text{CCH}_2$ ), 15.2 ( $\text{CCH}_3$ ) ppm. HRMS (EI)  $m/z$   $\text{C}_{14}\text{H}_{12}\text{O}_6$ , calcd.: 276.0684, found: 276.0686.

**SURMOF growth. Cu-DA-SBDC-dabco** – as previously described using the pump method. The experimental procedure used to grow MOFs on the organic surface has been discussed in some detail previously.<sup>3,4,5,6</sup> In short, for Cu-DA-SBDC-dabco the epitaxial growth process consisted of alternately immersing a 11-mercaptoundecanol (MUD) terminated SAM substrate into ethanolic solutions of the building units: copper acetate and  $\text{H}_4\text{-DA-SBDC}$  / dabco (equimolar ratio). Between each immersion step, the substrates are rinsed thoroughly with ethanol. In the present work, the SAM substrates were immersed into 1 mM ethanolic solution of copper acetate for 15 min, subsequently rinsed with pure ethanol solution for 2 min, and then immersed into  $\text{H}_4\text{-DA-SBDC}$  / dabco (equimolar ratio) solutions for 30 min. All the solutions were kept at 50 °C during MOF thin film preparations.

**SURMOF growth. Cu-DA-SBDC** – as previously described using the spray method. The SURMOF-2 samples were grown on Au substrates (100-nm Au/5-nm Ti deposited on Si wafers) using a high-throughput approach, spray method.<sup>7</sup> The gold substrates were functionalized by self-assembled monolayers, SAMs, of 16-mercaptohexadecanoic acid (MHDA). These substrates were mounted on a sample holder and subsequently sprayed with a 1 mM solution of  $\text{Cu}_2(\text{CH}_3\text{COO})_4 \times \text{H}_2\text{O}$  in ethanol and an ethanolic solution 0.1 mM of DA-SBDC at room temperature. The number of spray cycles employed was 20. After synthesis all samples were characterized with X-ray diffraction (XRD).

**Computational methods.** Initial structures were created using a preliminary version of our framework creator, which allows the creation of framework structures by specification of the component secondary building units. Structures were subsequently optimized using the General Utility Lattice Program (GULP) version 4.08.<sup>8,9</sup> The bond order specified between paddlewheel Cu atoms was 0.5, Cu-O was also specified as 0.5, all other bond orders were specified

according to standard chemical notation. Pore size characterization of the SURGEL samples used for the arabinose loading experiments was performed using Sarkisov's PoreBlazer v3.0.2: Sarkisov and Harrison, Computational structure characterization tools in application to ordered and disordered porous materials, Molecular Simulation, Vol 37, Issue 15, pages 1248-1257, 2011.<sup>10</sup> The Pore limiting diameter was determined from the theoretical model and amounts to 5.05 Å and the maximum pore diameter amounts to 7.03 Å. The pore size before the crosslinking amounts to 9.67 Å.

**Cross-linking reaction.** Freshly prepared samples of Cu-DA-SBDC and Cu-DA-SBDC-dabco were immersed in a solution of toluene containing 1mg/mL cross-linker. The samples were then heated in the solution for 7 d in dark at 80 °C under a nitrogen atmosphere. Afterwards the samples were thoroughly rinsed with acetone and ethanol and dried under nitrogen flow.

**Conversion of cross-linked SURMOF into SURGEL.** Cross-linked SURMOF samples were immersed in 10 mL ethanol/water 1/1 (volume) containing 1 mg ethylene diaminetetraacetic acid (EDTA). After 30 min immersion at room temperature, the samples were rinsed thoroughly with ethanol and water and dried under nitrogen flow.

**Loading of SURGEL with arabinose.** Cu-DA-SBDC based SURGEL samples were immersed in 5 mL solution of arabinose in water (1% w) for 3 d at room temperature. Afterwards the samples were rinsed with water and dried under nitrogen flow.

**Bacterial strains and culture conditions.** *Escherichia coli* DH5α (Invitrogen) and *Pseudomonas putida* KT2440 (DSM 6125) were routinely grown in Luria-Bertani (LB) broth or M9 minimal medium<sup>11</sup> at 37 °C for *E. coli* and 30 °C for *P. putida* with vigorous aeration. Gentamicin was added for plasmid selection and maintenance at 10 µg/mL for *E. coli* and 30 µg/mL for *P. putida* KT2440.

**Construction of *E. coli* pJN::GFP and *P. putida* pJN::GFP.** The green fluorescent protein (GFP) was used as a gene expression reporter system to study targeted gene expression in bacterial cells. For these analyses, plasmid pJN::GFP containing the *gfp* gene under the L-arabinose-inducible araBAD promoter was constructed. To form this plasmid, the *gfp* gene was amplified by PCR using EcoRI and XbaI flanked oligonucleotides and plasmid pProbe-AT' harboring the *gfp* gene<sup>12</sup> as template DNA, and subsequently cloned co-linear to the araBAD promoter in pJN105<sup>13</sup> to create pJN::GFP. The plasmid pJN::GFP was transferred to *E. coli* DH5α and *P. putida* KT2440 by electroporation resulting in strains *E. coli* pJN::GFP and *P. putida* pJN::GFP.

**GFP gene expression analyses.** Overnight grown bacterial cultures of *E. coli* pJN::GFP and *P. putida* pJN::GFP were diluted 1:100 in fresh LB or M9 broth medium, respectively, and inoculated in petri dishes containing SURGEL samples with and without arabinose for several hours to allow bacterial adherence and biofilm formation. The microscopic analysis of bacteria on the SURGEL surfaces and *gfp* gene expression demonstrated by the presence of the GFP protein within the bacterial cell was performed with an Axioplan 2 imaging fluorescence

microscope (Carl Zeiss) and images were captured and processed with AxioVision software. To visualize all viable bacteria on the SURGEL samples without arabinose, cells were stained using 5-cyano-2,3-ditolyl tetrazolium chloride (CTC) as described previously.<sup>14</sup>

- (1) Barral, K.; Moorhouse, A. D.; Moses, J. E. *Organic Letters* **2007**, 9, 1809-1811.
- (2) Gorman, I. E.; Willer, R. L.; Kemp, L. K.; Storey, R. F. *Polymer* **2012**, 53, 2548-2558.
- (3) Liu, J.; Lukose, B.; Shekhah, O.; Arslan, H. K.; Weidler, P.; Gliemann, H.; Bräse, S.; Grosjean, S.; Godt, A.; Feng, X.; Mullen, K.; Magdau, I.-B.; Heine, T.; Wöll, C. *Sci. Rep.* **2012**, 2.
- (4) Shekhah, O.; Wang, H.; Kowarik, S.; Schreiber, F.; Paulus, M.; Tolan, M.; Sternemann, C.; Evers, F.; Zacher, D.; Fischer, R. A.; Wöll, C. *Journal of the American Chemical Society* **2007**, 129, 15118-15119.
- (5) Shekhah, O.; Liu, J.; Fischer, R. A.; Wöll, C. *Chemical Society Reviews* **2011**, 40, 1081-1106.
- (6) Shekhah, O.; Arslan, H. K.; Chen, K.; Schmittl, M.; Maul, R.; Wenzel, W.; Wöll, C. *Chemical Communications* **2011**, 47, 11210-11212.
- (7) Arslan, H. K.; Shekhah, O.; Wohlgemuth, J.; Franzreb, M.; Fischer, R. A.; Wöll, C. *Advanced Functional Materials* **2011**, 21, 4228-4231.
- (8) Gale, J. D. *Zeitschrift für Kristallographie - Crystalline Materials* **2005**, 220, 552-554.
- (9) Gale, J. D.; Rohl, A. L. *Molecular Simulation* **2003**, 29, 291-341.
- (10) Sarkisov, L.; Harrison, A. *Molecular Simulation*, 2011, 37, 1248-1257.
- (11) Breidenstein, E. B. M.; Janot, L.; Strehmel, J.; Fernandez, L.; Taylor, P. K.; Kukavica-Ibrulj, I.; Gellatly, S. L.; Levesque, R. C.; Overhage, J.; Hancock, R. E. W. *PLoS ONE* **2012**, 7, e49123.
- (12) Miller, W. G.; Leveau, J. H. J.; Lindow, S. E. *Molecular Plant-Microbe Interactions* **2000**, 13, 1243-1250.
- (13) Newman, J. R.; Fuqua, C. *Gene* **1999**, 227, 197-203.
- (14) Li, J.; Kleintschek, T.; Rieder, A.; Cheng, Y.; Baumbach, T.; Obst, U.; Schwartz, T.; Levkin, P. A. *ACS Applied Materials & Interfaces* **2013**, 5, 6704-6711.

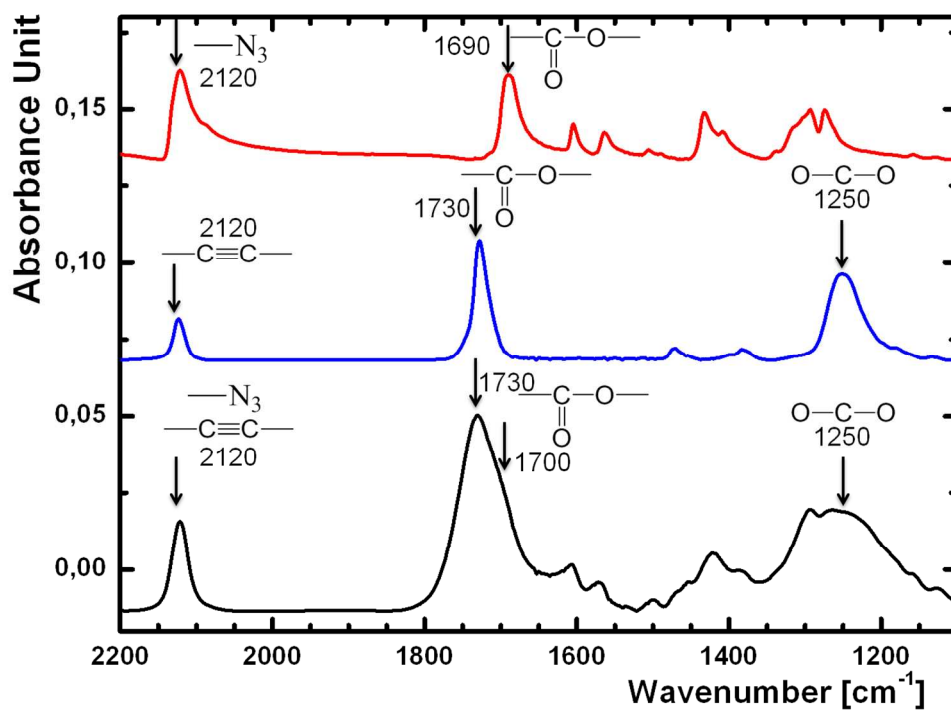


Figure S1. IRRAS spectra of the free linker DA-SBDC (red), the cross-linker (blue) and the cross-linked Cu DA-SBDC SURMOF-2 after EDTA treatment (black).

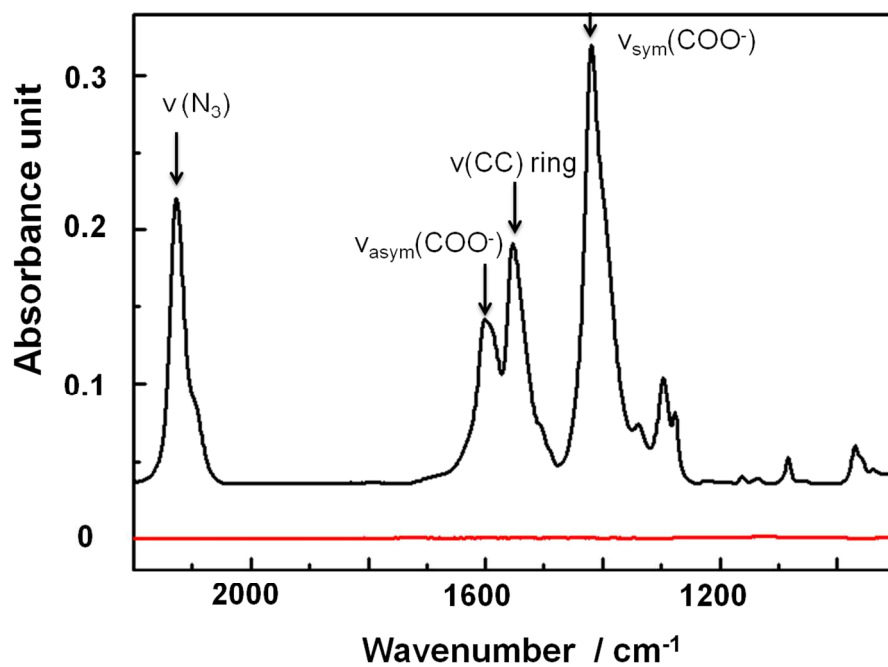


Figure S2. IRRAS spectra of the Cu DA-SBDC SURMOF-2 before EDTA (black), and after EDTA treatment (red) showing the complete removal of the non-cross-linked SURMOF under these conditions.



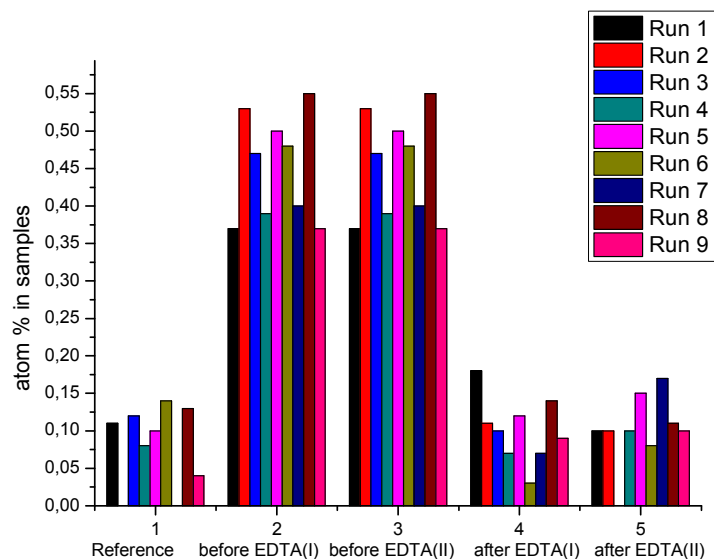


Figure S3. Atom % of copper by EDX analysis of (1) a blank gold reference substrate, (2) cross-linked SURMOF-2 sample 1 before EDTA treatment, (3) cross-linked SURMOF-2 sample 2 before EDTA treatment, (4) cross-linked SURMOF-2 sample 1 after EDTA treatment, (5) cross-linked SURMOF-2 sample 2 after EDTA treatment.

For each sample 9 spots were selected for analysis, indicated as runs 1-9.

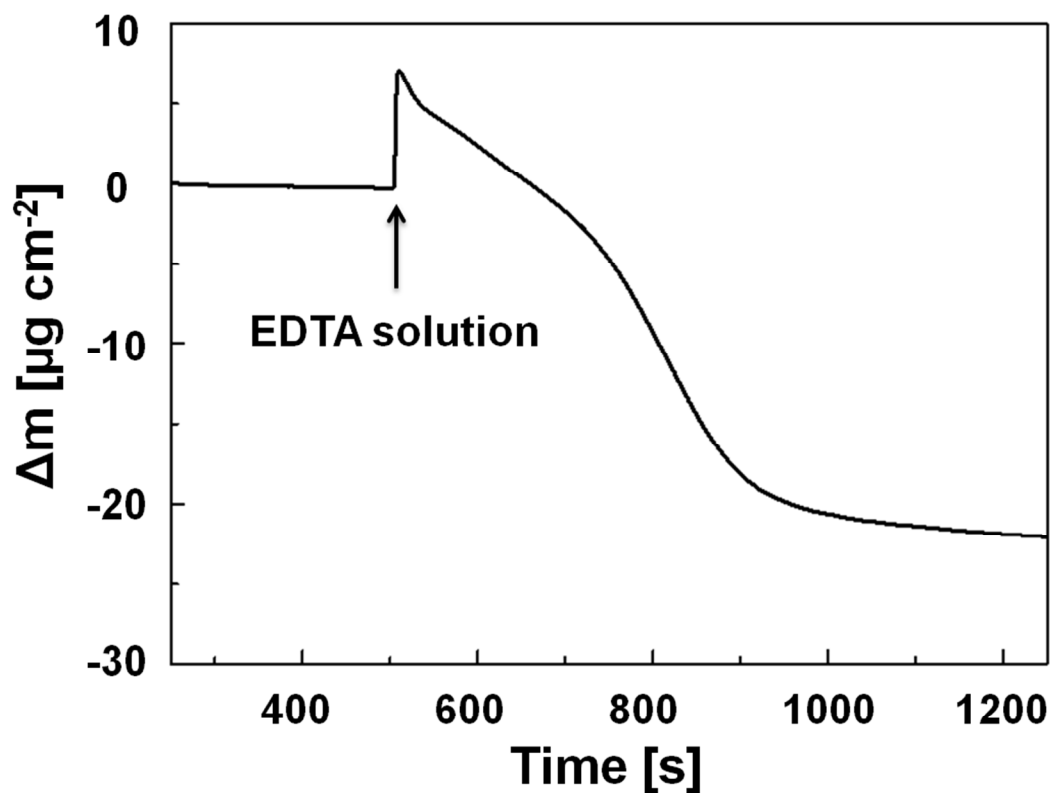


Figure S4. In situ QCM-D study of copper ion removal by EDTA in EtOH/H<sub>2</sub>O. The cross-linked SURMOF-2 coated QCM substrate (preparation as described for other gold substrates) was equilibrated in EtOH at 25 °C. At  $t = 480$  s a saturated EDTA solution in H<sub>2</sub>O/EtOH 1/1 %V was introduced into the flow chamber, leading to the removal of copper ions. The QCM responds shows an initial frequency decrease (weight uptake) caused by adsorption of EDTA molecules on the substrate followed by a frequency increase (weight loss) caused by the removal of the copper ions. The IRRAS spectrum after the QCM measurement (Figure S5) shows the typical characteristics of the cross-linked SURMOF-2 after EDTA treatment as shown in Figure S1 and Figure 2 (c) in the main text.

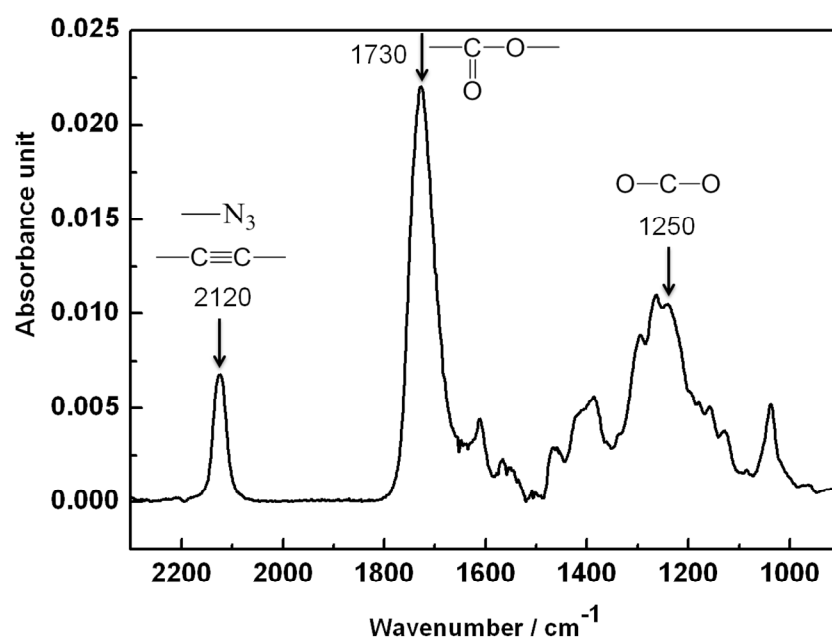


Figure S5. IRRAS spectrum of the SURGEL coated QCM substrate after EDTA treatment.

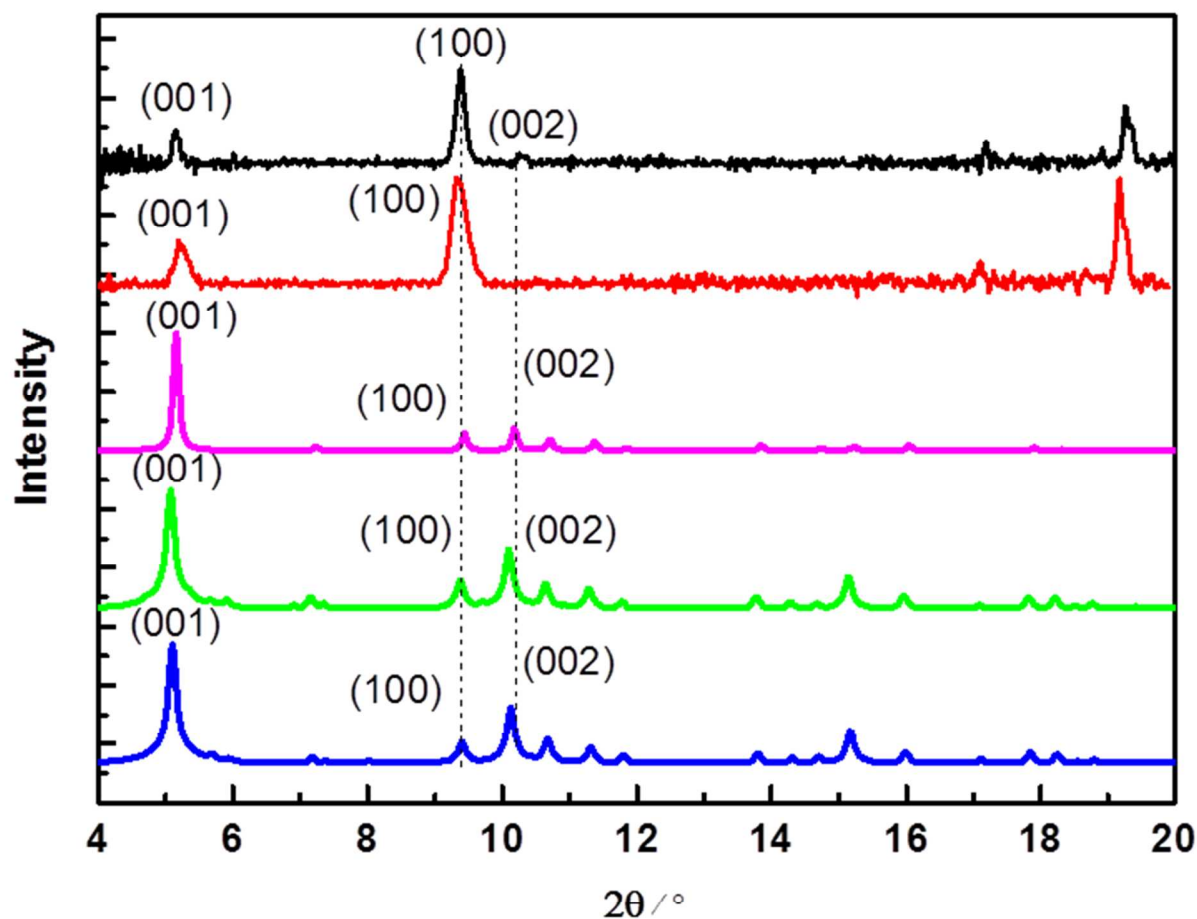


Figure S6. Experimental XRD data of a pillared-layer Cu-DA-SBDC-dabco SURMOF before (top, black), after cross-linking (second, red) and simulated XRD data for powder samples of the Cu-DA-SBDC-dabco MOF before cross-linking (third, pink), after cross-linking within one plane (fourth, green) and after cross-linking between two adjacent planes (bottom, blue). The XRD data suggests a preferential [100] orientation of the SURMOF perpendicular to the substrate.

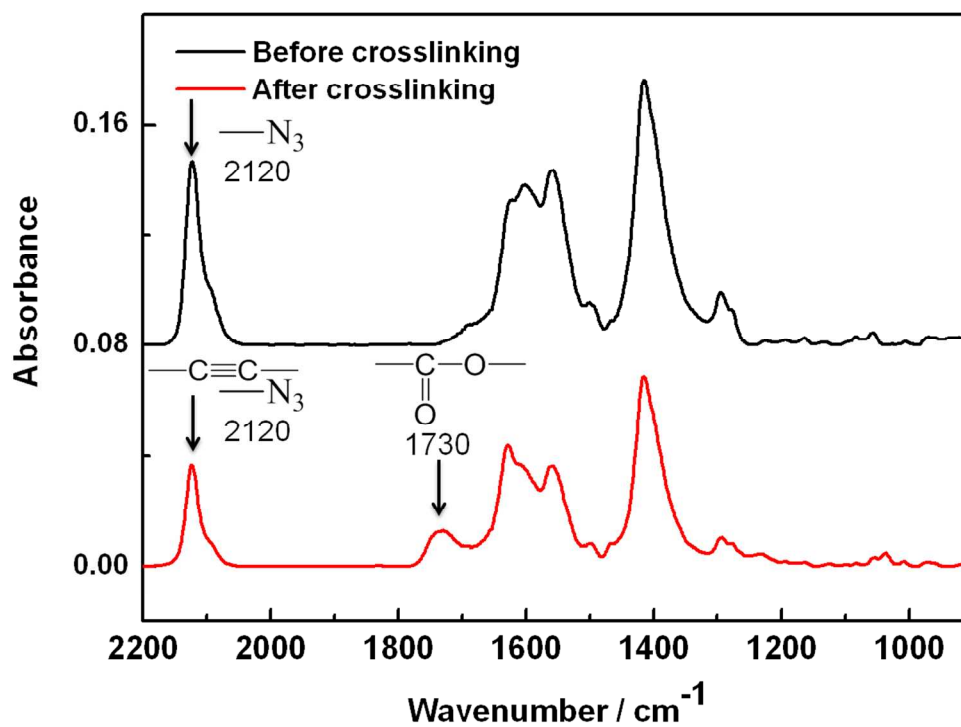


Figure S7. IRRAS spectra of a pillared-layer Cu-DA-SBDC-dabco SURMOF before (top, black) and after cross-linking (bottom, red).

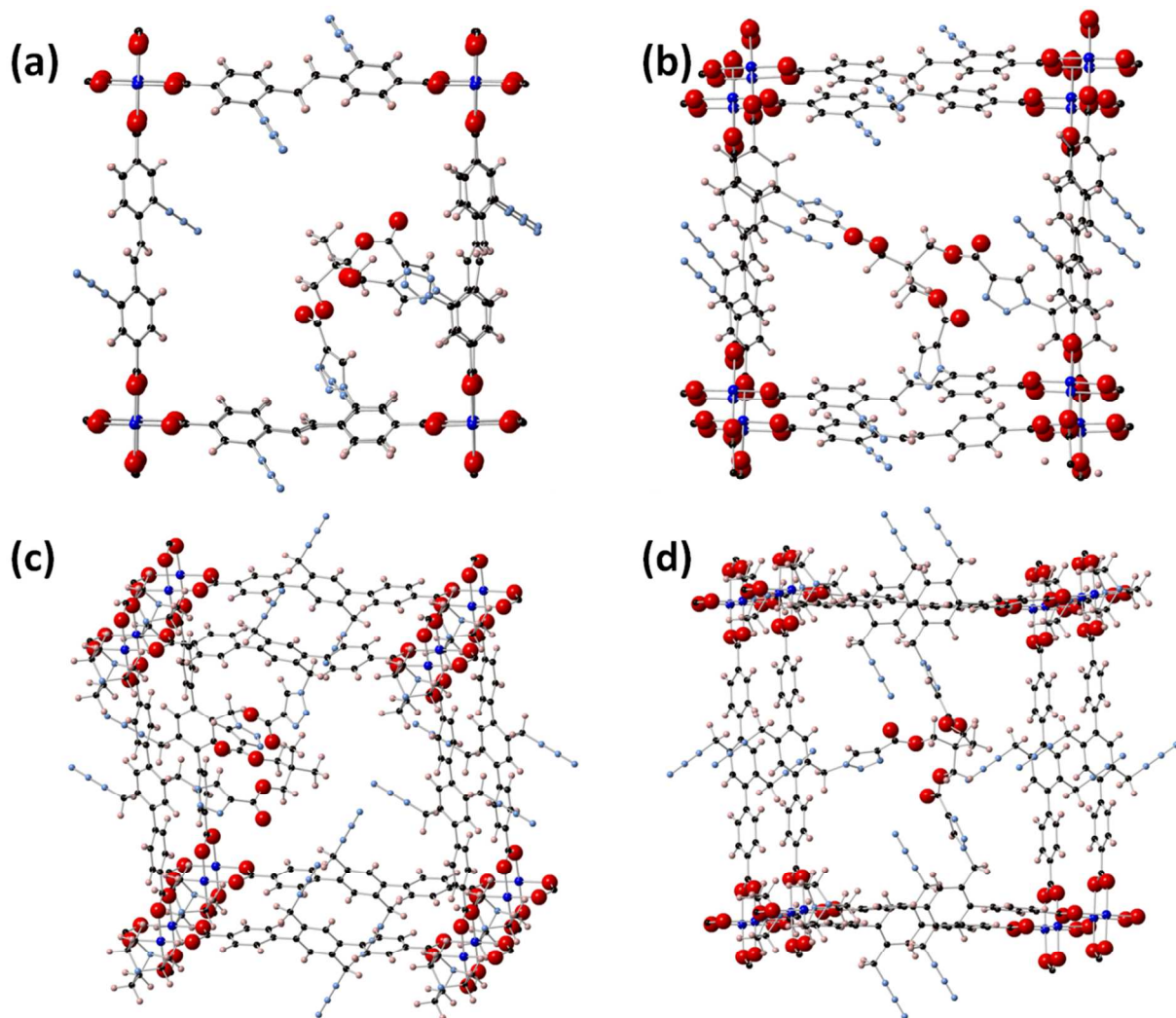
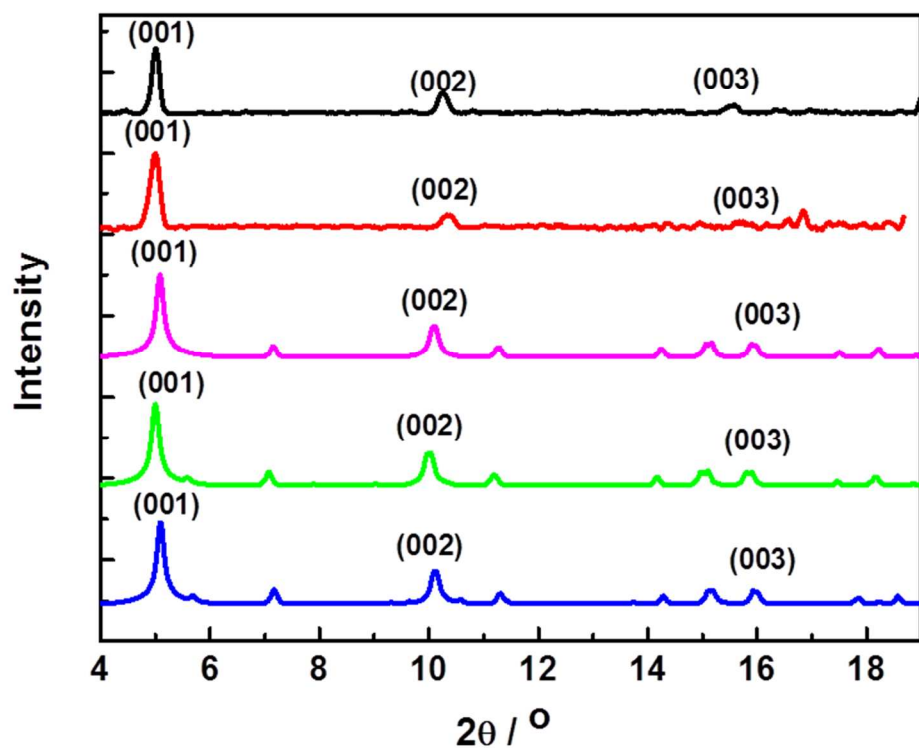


Figure S8. Simulated structures of cross-linked SURMOFs. (a) SURMOF-2 Cu-DA-SBDC cross-linked between two layers; (b) SURMOF-2 Cu-DA-SBDC cross-linked within one layer; (c) pillared-layer SURMOF Cu-DA-SBDC dabco cross-linked between two layers; (d) pillared-layer SURMOF Cu-DA-SBDC dabco cross-linked within one layer.



S9 Experimental XRD data of Cu-DA-SBDC SURMOF-2 before cross-linking (top, black), after cross-linking (second, red) and simulated XRD data for powder samples of the Cu-DA-SBDC MOF before cross-linking (third, pink), after cross-linking within one plane (fourth, green) and after cross-linking between two adjacent planes (bottom, blue). The XRD data suggests a preferential [001] orientation of the SURMOF perpendicular to the substrate.

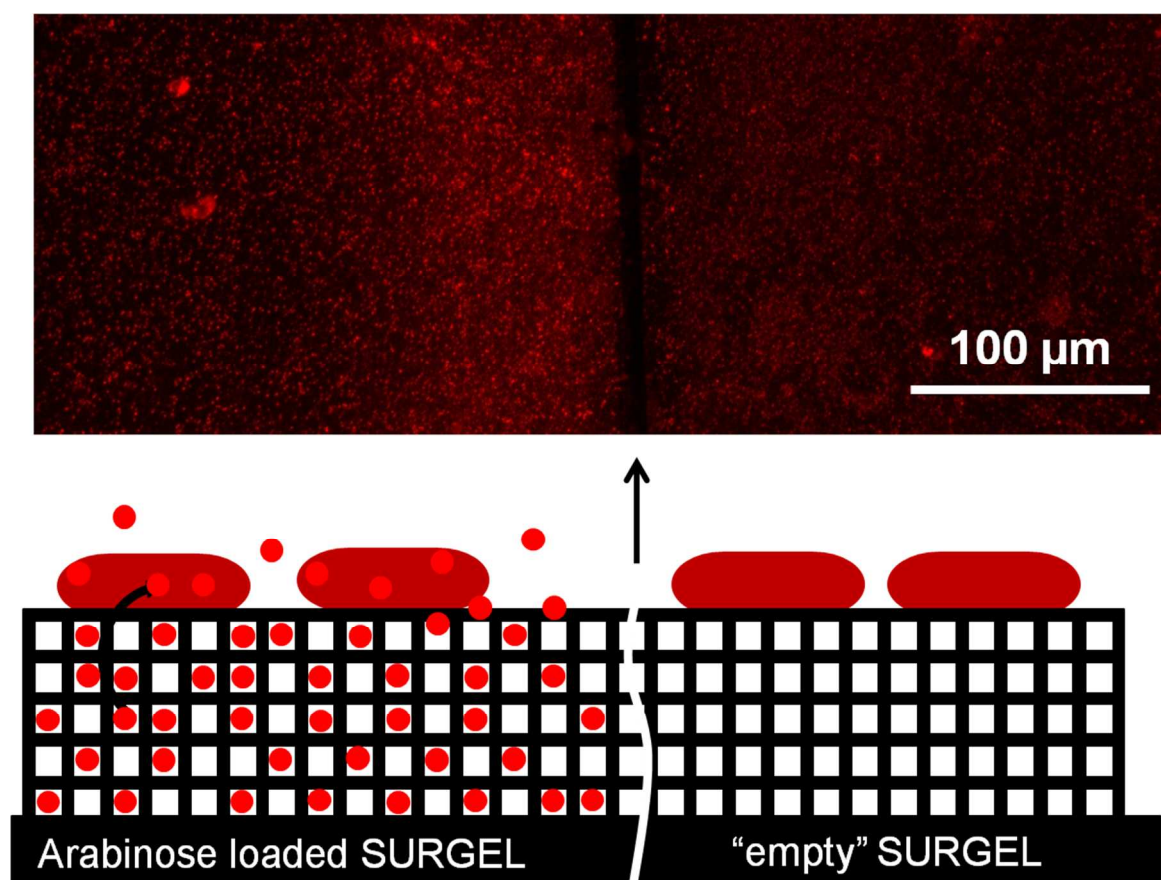


Figure S10. Fluorescent microscopy images of *P. putida* pJN::GFP after 24 h incubation in presence of arabinose loaded SURGELs (bottom) and empty SURGEL (top). The bacteria were stained using 5-cyano-2,3-ditolyl tetrazolium chloride (CTC) showing that both substrates contained bacteria settled on the SURGEL substrates.



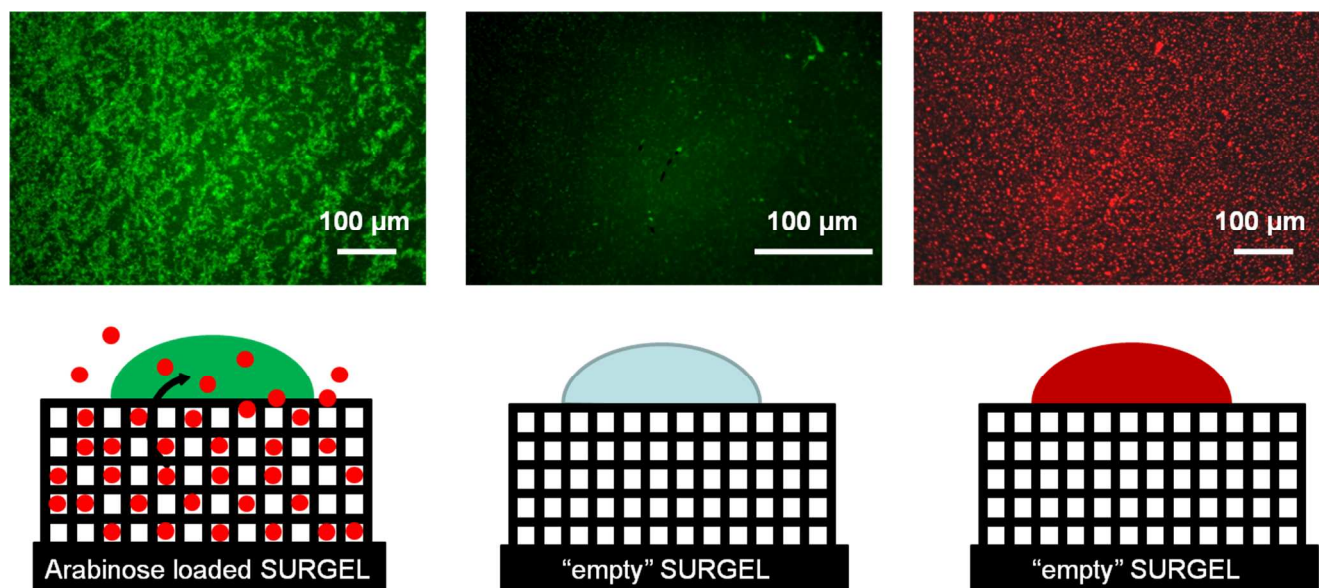


Figure S11. Fluorescent microscopy images of *E. coli* pJN::GFP after 24 h incubation in presence of arabinose loaded SURGELs (left) and empty SURGEL (middle). Afterwards the bacteria settled on the empty SURGEL substrate were stained using 5-cyano-2,3-ditolyl tetrazolium chloride (CTC) showing that also for the “empty” sample bacteria settled on the SURGEL substrate.

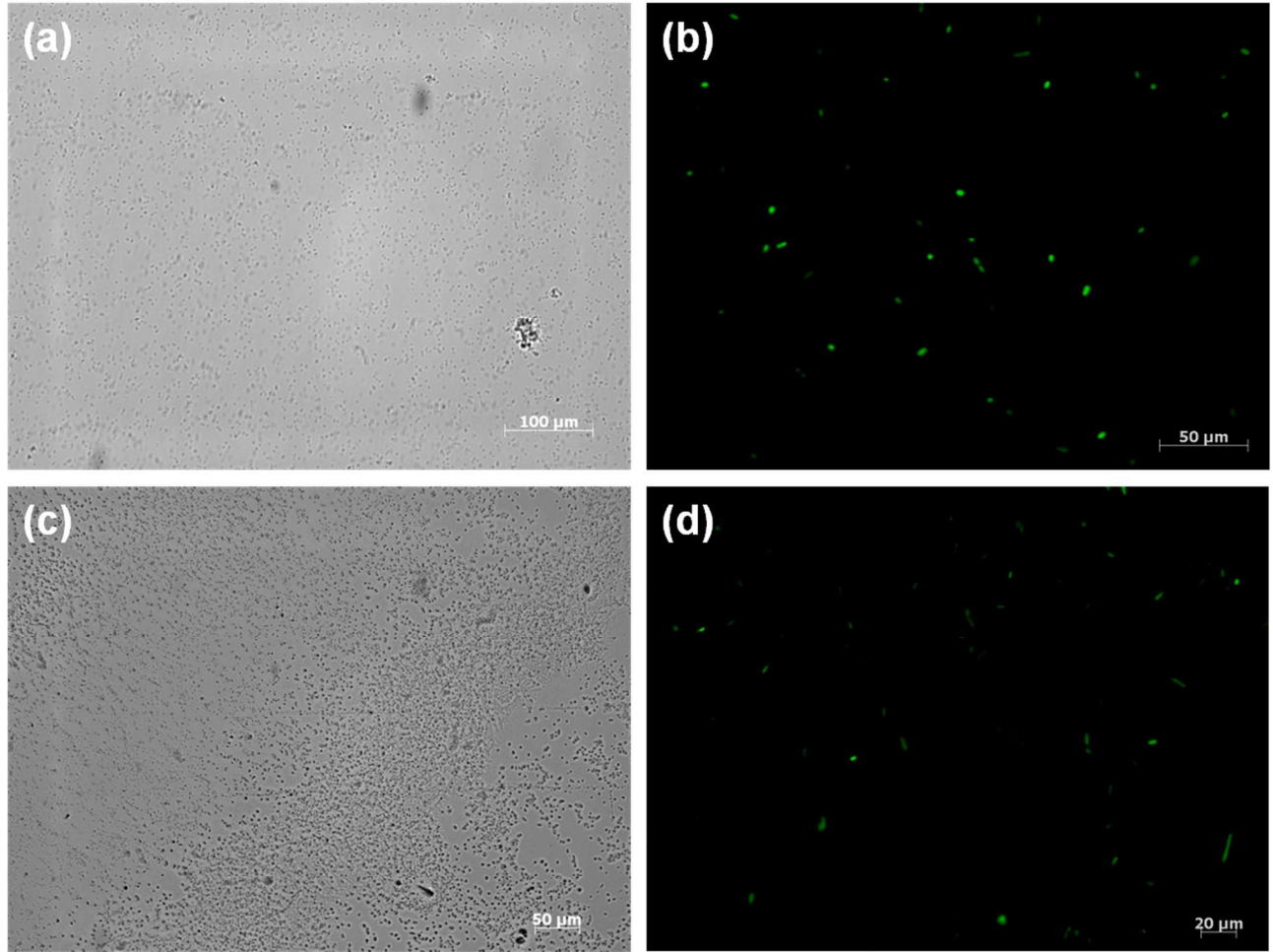


Figure S12. Microscopy images from the broth supernatant of both bacteria organisms after 24 h incubation in presence of arabinose loaded SURGELS. (a) Bright field image of *P. putida* pJN::GFP, (b) fluorescent microscopy image of *P. putida* pJN::GFP, (c) bright field image of *E. coli* pJN::GFP and (d) fluorescent microscopy image of *E. coli* pJN::GFP.

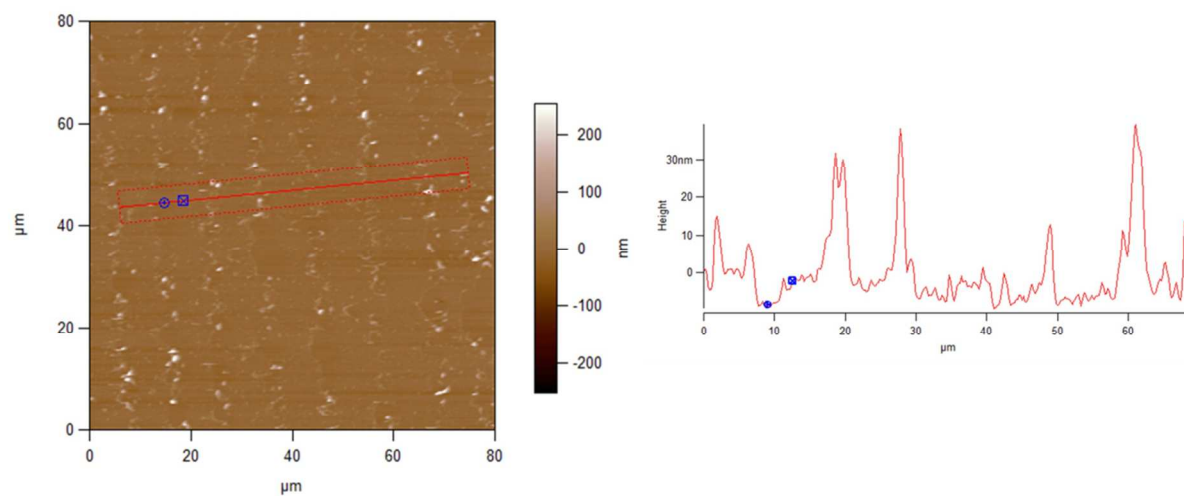


Figure S13. Atomic Force Microscopy (AFM) image of a patterned Cu-DA-SBDC-dabco SURGEL sample after delamination in basic conditions.